

STATUS OF LASA-INFN R&D ACTIVITY ON PIP-II LOW-BETA PROTOTYPES

M. Bertucci*, A. Bosotti, A. D'Ambros, E. Del Core, A. T. Grimaldi, P. Michelato,
L. Monaco, C. Pagani¹, R. Paparella, D. Sertore, INFN LASA, Segrate (MI), Italy
A. Gresele, Zanon Research & Innovation, Schio (VI), Italy
¹also at Università degli Studi di Milano, Milano (MI), Italy

Abstract

INFN LASA is developing some PIP-II $\beta = 0.61$ cavity prototypes so to setup a high-Q recipe allowing to reach the PIP-II performance target in view of the series production. A single cell cavity was treated with a baseline recipe, whereas a multicell cavity underwent a mid-T bake step as final surface treatment. Both cavities were then tested at the LASA vertical experimental facility. The test results are here reported and discussed. Basing on the satisfactory results so far obtained, a strategy for the qualification and upgrade of the LASA vertical test facility is outlined.

INTRODUCTION

INFN LASA is appointed to build 40 650 MHz $\beta = 0.61$ superconducting cavities that will constitute the low-beta (LB) section of the PIP-II Linac. Specifications for operation in the machine are $E_{acc} = 16.9 \text{ MV m}^{-1}$ with a $Q_0 \geq 2.4 \cdot 10^{10}$. Given such challenging target, the treatment recipe has been based on Electropolishing (EP) as main surface removal treatment. The bulk EP will be the starting point of a so-called “high-Q” surface recipe.

The definition of the whole treatment sequence is under way. In parallel with the activities carried out at FNAL [1], INFN-LASA is conducting an analogous R&D effort, on single and multi-cell cavity prototypes, manufactured at the company Zanon Research & Innovation Srl. Some of the cavities were shared with FNAL, in sake of a joint effort on many technical issues that need to be addressed. The final goal is the definition of the specifications for the fabrication of the forthcoming cavity series production.

PROTOTYPES TREATMENT VALIDATION STRATEGY

The first phase of the treatment optimization activity consisted on the setup of the Electropolishing plant operating at the company Zanon Research & Innovation Srl. The facility is the same employed in the series production of XFEL [2] and LCLS-II [3] 1.3 GHz superconducting cavities. Due to the different size and geometry of PIP-II LB cavities, the treatment parameters were finely tuned by several short EP trials carried out on the single-cell prototype B61S-EZ-002 so to optimize smoothness, removal rate and iris/equator removal ratio [4]. Pivotal was the installation of Aluminum cathode enlargements in correspondence of the cells, which noticeably increased the current density at the equators.

Afterwards, the activity proceeded with the definition of a baseline treatment recipe, which served as a reference for the forthcoming treatments. Among the various recipes which are nowadays available, the so-called mid-T bake [5] and the 2/0 nitrogen doping [6] were chosen as possible candidates, since they guarantee high-Q operation at a medium accelerating field. The aforementioned recipes are discussed here in the specific case of the PIP-II 650 MHz LB cavity.

The Baseline Recipe

The baseline recipe was applied on the single cell cavity B61S-EZ-002. The treatment steps went along the same lines of the XFEL 1.3 GHz cavity production, in the “final EP” scheme. At first, a bulk EP of 150 μm removed the damaged layer on the inner RF surface. Then, the cavity was heat treated at 800 $^{\circ}\text{C}$ for 2 hours to degas the hydrogen adsorbed by the Niobium during the fabrication and the surface treatment. After this, the cavity proceeded with a 25 μm final EP. Differently to XFEL, the “cold” EP regime was adopted. In this variant, a lower acid temperature (around 8 $^{\circ}\text{C}$) is used so to yield a lower average temperature on cavity surface (around 12 $^{\circ}\text{C}$). Cold EP allows to obtain a smoother surface and a more uniform removal over the cavity [7], therefore limiting non-linear losses increasing power dissipation at higher fields [8]. Eventually, the baseline recipe ended with the low temperature baking (48 hours at 120 $^{\circ}\text{C}$ in UHV conditions), whose goal is to get rid of the high-field Q-slope.

The Nitrogen Doping Recipe

Nitrogen doping allows to obtain high Q values at medium accelerating fields, and it has been applied with success during the LCLS-II cavity production. Anyway, some issues emerged in the case of 650 GHz LB cavities [1]. The anti-Q slope typical of 1.3 GHz cavities is absent even though a decrease in BCS surface resistance is evident. On the other side, an increase in residual resistance was also noticed, due to an increase in trapped flux sensitivity. A $T > 900^{\circ}\text{C}$ annealing is needed to recover the magnetic flux properties of the material. This in turn may affect the mechanical stability of the cavity. The impact of these issues on the cavity operation in the cryomodule is under investigation.

The first trials of doping performed by FNAL confirmed that nitrogen doping recipe enables higher Q operation w.r.t. baseline treatments. INFN-LASA will apply the same recipe on the B61S-EZ-003 single cell cavity. After a bulk EP treatment of 150 μm , the cavity will be annealed in UHV at

* michele.bertucci@mi.infn.it

900 °C for 3 hours. Then, the temperature will be ramped down to 800 °C to perform the nitrogen doping procedure in the so called “2/0” scheme. This consists of a 2 min nitrogen injection at a 25 mTorr pressure without any soak period before the ramp-down to room temperature. Eventually, the cavity will proceed with a final cold EP. The final removal amount is essential so to perfectly tune the nitrogen interstitial concentration at the RF surface. Due to the different shape and size, this value is expected to be different from the LCLS-II case. The definition of the optimum removal is currently under investigation.

The Mid-T Bake Recipe

Aiming to find an alternative high-Q treatment, the mid-T bake recipe was chosen. This recipe has been successfully employed [5, 9] with outstanding performances in terms of Q_0 values at low and medium fields, also for 650 MHz cavities [10], even though the impact of such treatment on the residual resistance is still under study. This recipe was applied on the multicell B61-EZ-002 cavity.

Such recipe started with the same sequence of operations of the baseline, up to the final cold EP. Afterwards, the cavity is baked at 300 °C for 3 hours under UHV, so to allow the redistribution of oxygen content in the subsurface layer, which inhibits the hydride segregation which would introduce additional losses in the RF layer [11]. After that, the cavity was exposed to air so to allow the regrowth of the Nb_2O_5 layer. No additional surface removal has to be performed, so to not affect the oxygen profile. Particular care was therefore undertaken to preserve surface cleanliness during the 300 °C bake itself and on the following preparation steps.

The status of INFN LASA experimental activity on PIP-II prototypes is summarized in Table 1. In addition to what already stated, a mid-T bake treatment is foreseen on the baseline-treated single cell B61S-EZ-002, with a higher annealing temperature (900 °C). Multi-cell cavity B61S-EZ-002 will instead undergo a complete jacketing procedure so to validate the fabrication sequence up to installation in the cryomodule. The fate of cavity B61-EZ-003 will depend upon its experimental performances.

VERTICAL TEST RESULTS

After the treatment, cavity B61S-EZ-002 and B61-EZ-002 were tested in INFN LASA vertical test facility. The cryostat allows to reach temperatures as low as 1.5 K. The cavity test stand is equipped with diagnostics for quench events (second sound, fast thermometry) and field emission (photodiodes, external proportional counter and NaI scintillator) [12]. Typical cooldown rate is around 1 K min⁻¹ so the residual magnetic field (max. 8 mG) in the cryostat inner volume is expected to be completely trapped.

The vertical test result for single cell cavity B61S-EZ-002 is shown in Fig. 1. In the first test at 2 K the cavity reached 30 MV m⁻¹, with high-field Q-slope and moderate field emission (FE in the following) starting at 15 MV m⁻¹. In order to mitigate FE, a 40 min RF processing w carried

Table 1: Prototype Cavities Processing Strategy

Cavity	1st treatment	2nd treatment
B61S-EZ-002 (single cell)	“Baseline”: 150 μm bulk EP 800 °C 2h HT 25 μm cold EP 120°C 48h bake	“Mid-T bake”: 30 μm bulk EP 900 °C 3h HT 5 μm cold EP 300 °C 3h bake
B61-EZ-002 (multi-cell)	“Mid-T bake”: 150 μm bulk EP 800 °C 2h HT 5 μm cold EP 300 °C 3h bake	“Jacketing” : Tank welding with full diagnostics equipment
B61S-EZ-003 (single cell)	“N ₂ doping”: 150 μm bulk EP 900 °C 2h HT 2/0 N ₂ @ 800 °C 7 μm cold EP	to be planned

out. The test was then repeated, and a slight degradation of Q_0 at high fields was noticed, together with the increase of radiation of an order of magnitude. This behavior is probably due to a change in the emitter topology induced by local RF heating. By fitting these radiation data with the Fowler-Nordheim law, one indeed obtains $\beta = 120$ and $\beta = 180$ field enhancement factors for the first and second test, respectively.

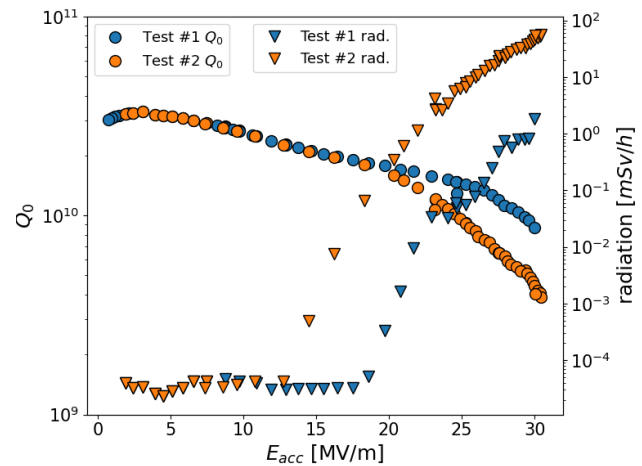


Figure 1: Q_0 vs E_{acc} for single cell B61S-EZ-002 before and after high-field RF processing. The radiation level is also shown on the secondary axis.

The vertical test result for multi-cell cavity B61S-EZ-002 is shown in Fig. 2. In the first test at 2 K the cavity experienced some multipacting activity between 7 and 12 MV m⁻¹, associated with radiation. Then, the behavior suddenly changed just above 20.8 MV m⁻¹, with the abrupt rise of radiation and a Q-degradation. The test was then repeated again from low fields so to avoid He-bath instabilities. At first,

this second rise followed the same trend of the previous one. Then, the radiation started to rise from 14 MV m^{-1} , with a simultaneous drop of the Q_0 . The radiation level exponentially increased up until the cavity quenched, at 23 MV m^{-1} . This can be explained assuming the irreversible activation of a field emitter induced by RF heating at high fields. Such mechanism has been already described in [13]. Comparing

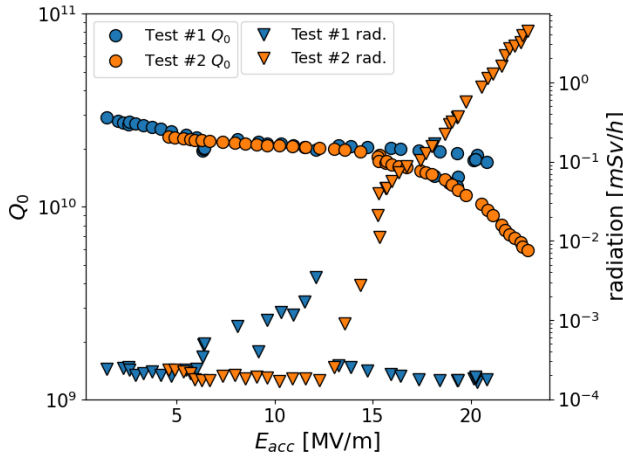


Figure 2: Q_0 vs E_{acc} for multi-cell B61-EZ-002 before and after emitter activation. The radiation level is also shown on the secondary axis.

the two curves shown in Fig. 2, one can state that the Q-variation at a given field level is due to the power dissipated in electron current, P_{FE} , which is drained from the RF field in the cavity. This contribution adds to the power dissipated by cavity walls, P_d , so that the overall dissipated power becomes $P'_d = P_d + P_{FE}$. Hence, the Q_0 in presence of FE is given by $Q'_0 = \frac{(E_{acc}l)^2}{\frac{R}{Q}P'_d}$. Rearranging, one obtains:

$$\frac{1}{Q'_0} = \frac{1}{Q_0} + \frac{\frac{R}{Q}P_{FE}}{(E_{acc}l)^2} \quad (1)$$

Where Q_0 refers to the first test (no FE) and Q'_0 to the second (with FE). P_{FE} is a function of E_{acc} and, considering energy conservation, can be calculated as $P_{FE} = \frac{1}{T_{RF}} \sum E_k$, namely the sum of the impact energies of electrons emitted in a RF cycle divided by the RF period.

Basing on these considerations, the impact of FE has been modeled by a simulation based on *Fishpact* [14] code. More details on the program will be given in a future article. The experimental data reported in Fig. 2 were used to evaluate the FE contribution to the Q drop in the second test due to the emitter activation. A $\beta=300$ field enhancement factor was derived by fitting the dose rate vs E_{acc} with the Fowler-Nordheim law. Such value has been used to reconstruct the FE-generated electron pattern for every E_{acc} value, by probing different emission sites until a matching between simulated electron impact energies and the X-ray spectrum measured by the scintillator is found. The calculated overall power P_{FE} was then used to reconstruct the second test

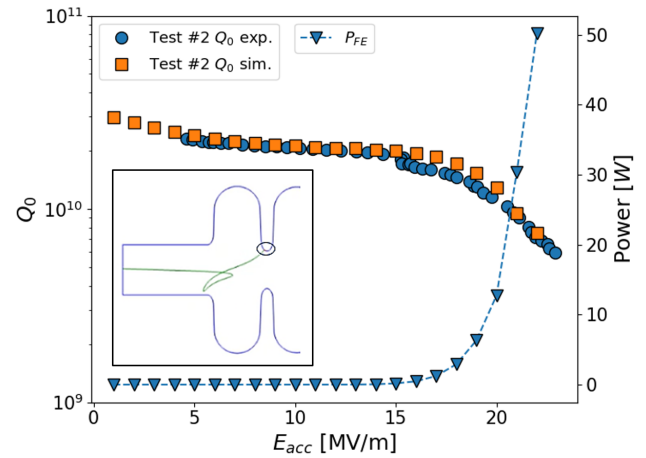


Figure 3: experimental and simulated Q_0 vs E_{acc} for cavity B61-EZ-002 test #2. The calculated P_{FE} is plotted on the secondary axis. The emitter position is shown in the insert.

curve Q'_0 starting from the first test Q_0 , by means of equation (1). Assuming an emitter surface of $S=1 \times 10^{-15} \text{ m}^2$ placed nearby iris 2, one obtains the calculated curve shown in Fig. 3. The resulting site is shown in the insert.

CONCLUSIONS

The R&D activity on PIP-II LB cavity prototypes at INFN LASA is ongoing. At the present day, a single cell cavity was processed by means of a baseline recipe and a multicell cavity was processed by a mid-T bake based recipe. In the next future, new surface treatments are planned. According to the experimental results here shown, cavity performances approach the qualification goal of $Q_0 \geq 2.4 \cdot 10^{10}$ at $E_{acc} = 16.9 \text{ MV m}^{-1}$. It must be stressed that the tests were done in a slow cooldown regime so that the Q-values are affected by the contribution of residual magnetic field. The future infrastructure upgrades are expected to boost these values above the qualification target.

REFERENCES

- [1] M. Martinello *et al.*, “Q-factor optimization for high-beta 650 MHz cavities for PIP-II”, *J. Appl. Phys.*, vol. 130, no. 17, p. 174501, 2021. doi:10.1063/5.0068531
- [2] W. Singer *et al.*, “Production of superconducting 1.3-GHz cavities for the European X-ray Free Electron Laser”, *Phys. Rev. Accel. Beams*, vol. 19, no. 9, p. 092001, 2016. doi:10.1103/PhysRevAccelBeams.19.092001
- [3] M. Rizzi, G. Corniani, A. Matheisen, and P. Michelato, “Comments on Electropolishing at Ettore Zanon SpA at the End of EXFEL Production”, in *Proc. 17th Int. Conf. RF Superconductivity (SRF'15)*, Whistler, Canada, Sep. 2015, paper MOPB102, pp. 394–398.
- [4] M. Bertucci *et al.*, “Electropolishing of PIP-II Low Beta Cavity Prototypes”, in *Proc. 19th Int. Conf. RF Superconductivity (SRF'19)*, Dresden, Germany, Jun.-Jul. 2019, paper MOP057, pp. 194–198. doi:10.18429/JACoW-SRF2019-MOP057

- [5] S. Posen, A. Romanenko, A. Grassellino, O.S. Melnychuk, and D.A. Sergatskov, “Ultralow Surface Resistance via Vacuum Heat Treatment of Superconducting Radio-Frequency Cavities” *Phys. Rev. Applied*, vol. 13, no. 1, p. 014024, 2020. doi:10.1103/PhysRevApplied.13.014024
- [6] Grassellino *et al.*, “Nitrogen and argon doping of niobium for superconducting radio frequency cavities: A pathway to highly efficient accelerating structures”, *Supercond. Sci. Technol.*, vol. 26, no. 10, p. 102001, 2013. doi:10.1088/0953-2048/26/10/102001
- [7] F. Furuta, D. Bice, A. C. Crawford and T. Ring, “Fermilab EP Facility Improvement”, in *Proc. 19th Int. Conf. RF Superconductivity (SRF’19)*, Dresden, Germany, Jun.-Jul. 2019, paper TUP022, pp. 453–455. doi:10.18429/JACoW-SRF2019-TUP022
- [8] K. Saito, “Surface Smoothness for High Gradient Niobium SC RF Cavities”, in *11th Workshop on RF Superconductivity (SRF’03)*, Lübeck/Travemünder, Germany, Sep 2003, paper THP15, pp. 637–640.
- [9] F. He *et al.*, “Medium-temperature furnace bake of Superconducting Radio-Frequency cavities at IHEP”, doi:10.48550/arXiv.2012.04817
- [10] S. Peng *et al.*, “Quality Factor Enhancement of 650 MHz Superconducting Radio-Frequency Cavity for CEPC”, *Appl. Sci.*, vol. 12, no. 1, p. 546, 2022. doi:10.3390/app12020546
- [11] A. Romanenko, F. Barkov, L. Cooley, and A. Grassellino, “Proximity breakdown of hydrides in superconducting niobium cavities”, *Supercond. Sci. Technol.*, vol. 26, p. 014024, 2012. doi:10.1088/0953-2048/26/3/035003
- [12] M. Bertucci *et al.*, “Quench and Field Emission Diagnostics for the ESS Medium-Beta Prototypes Vertical Tests at LASA”, in *Proc. 8th Int. Particle Accelerator Conf. (IPAC’17)*, Copenhagen, Denmark, May 2017, pp. 1007–1010. doi:10.18429/JACoW-IPAC2017-MOPVA061.
- [13] J. Knobloch, “Advanced thermometry studies of superconducting RF cavities”, Ph.D. Thesis, Phys. Dept. Cornell University, US, 1997.
- [14] G. Wu, M. Stirbet, H. Wang, R. Rimmer, and E. Donoghue, “Multipacting Analysis for JLAB Ampere Class Cavities”, in *Proc. SRF’05*, Ithaca, NY, USA, Jul. 2005, paper TUP28, pp. 300–302.